Polymerization of Olefins through Heterogeneous Catalysis. IX. Experimental Study of Propylene Polymerization over a High Activity $MgCl_2$-Supported Ti Catalyst

R. A. HUTCHINSON and W. H. RAY*

Department of Chemical Engineering, University of Wisconsin-Madison, Madison, Wisconsin 53706

SYNOPSIS

Results from an experimental study of propylene polymerization in heptane diluent over a high activity Mg-supported Ti catalyst are presented. The study provides an examination of the effect of operating conditions on polymerization rate, product melt index, and powder bulk density. Among the findings are that product bulk density decreases with increasing operating temperature and decreasing operating pressure while prepolymerization increases the bulk density. The results support the hypothesis that polymer morphology is closely linked to mass transfer limitations within the growing polymer particle during the early stages of polymerization.

INTRODUCTION

A major area of industrial interest in the field of heterogeneous catalyzed olefin polymerization is the control of particle morphology. The final form of the polymer product—particle shape and average size, particle size distribution (PSD), and bulk (or apparent) density of the powder—affects the downstream handling and processing of the polymer.[1,2] Control of polymer morphology is necessary in order to achieve good fluidization in gas phase reactors[3]; higher bulk density polymer also increases reactor throughput. With sufficient control over particle size and shape, it is possible to sell the reactor product directly; presently the majority of polyolefin powder is pelletized before shipping. Elimination of the pelletization step permits faster processing and less energy use.[4]

In general, polymer morphology is closely related to the morphology of the original catalyst particle, both in terms of shape and porosity.[5,6] Although replication of morphology is generally observed during polymerization, changes in particle porosity and structure do occur. For example, the mercury porosimetry data of Bukatov et al.[7] for propylene polymerization over a $TiCl_3$ catalyst show a decrease in particle void fraction from 0.46 to 0.21 as the polymerization proceeds to its final yield of 1350 g/g cat. Similarly, data from a Solvay patent[8] show that polypropylene particles with a bulk density of 0.45 g/cm^3 were produced from $TiCl_3$ catalyst particles with a bulk density of 0.9 g/cm^3 and a void fraction of 0.44. With the assumption that interparticle void fraction does not change during polymerization, a final polymer particle void fraction of 0.18 can be estimated.

Process conditions have an especially important effect on particle morphology during the initial stages of polymerization. For a high activity catalyst, a fivefold increase in particle diameter takes place in the first few minutes of polymerization, even though only 3–4% of the total polymer is produced during this time. For some catalysts, a high initial polymerization rate can lead to partial disintegration of the particles before individual catalyst fragments are bonded by polymer.[9,10] Controlling the initial growth is essential to maintain good particle morphology. It is hypothesized that uneven initiation of polymerization can even lead to the formation of hollow polymer particles, as shown schematically in Figure 1.[3]

For some catalysts, prepolymerization is often used to control initial growth rate and particle mor-

* To whom correspondence should be addressed.

Journal of Applied Polymer Science, Vol. 43, 1271–1285 (1991)
 CCC 0021-8995/91/071271-15$04.00

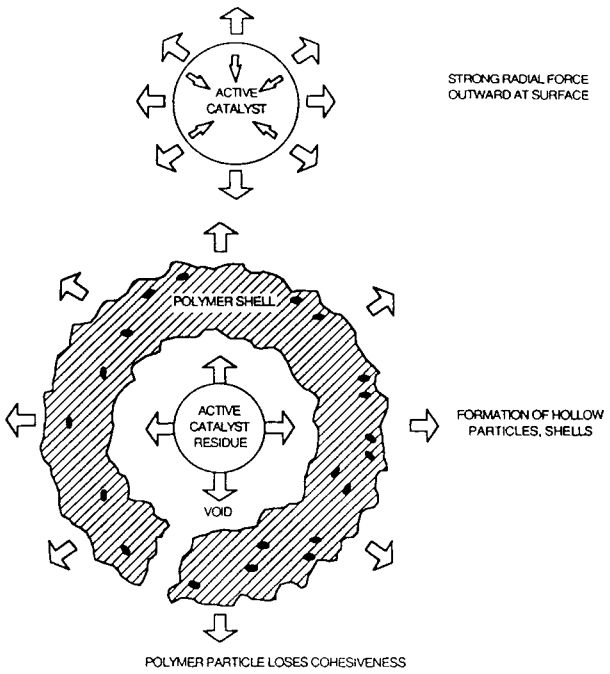

Figure 1 Schematic representation of poor polymer morphology caused by fast induction or uneven catalyst distribution. (Taken from Ref. 3.)

phology. A Hercules patent[2] reveals that particle morphology is improved when a prepolymerization step at room temperature and atmospheric pressure is used for a Mg-supported Ti catalyst. Both bulk density and average propylene polymerization rate increased with the addition of the prepolymerization step. Tang[11] also shows that prepolymerizing a Mg-supported Ti catalyst increases bulk density for both polypropylene and polyethylene particles. He suggests that the low growth rate during prepolymerization prevents excessive catalyst fragmentation and initiates a good replica relationship. However, some catalysts appear to maintain both high activity and control of particle morphology without prepolymerization. Zucchini and co-workers[12] claim that Montedison is able to obtain good polyethylene morphology at high rates of polymerization with the use of a Mg/Ti catalyst which has "controlled" breakup. No further details on catalyst structure were given.

In this paper, the effects of reactor operating conditions on particle morphology has been examined as part of a broader study involving the characterization of a high activity Mg-supported Ti catalyst used for propylene polymerization in heptane diluent. Data on reaction rates and polymer melt index are also presented. The results further elucidate the relationship between particle growth conditions and resulting polymer morphology.

EXPERIMENTAL

A schematic of the reactor system is shown in Figure 2. The stainless steel one gallon reactor, manufactured by Autoclave Engineers, has a variable speed motor to provide agitation. All experimentation is done at a stirring speed of 500 rpm using an eight-bladed 3.5-in. diameter impeller. Temperature is maintained by flowing cooling water through the internal coils at a constant flowrate, and using a PID Omega 149-737 controller connected to external band heaters. Control is generally to within 0.5°C of setpoint. After a reaction, slurry product is removed through the screw valve at the bottom of the reactor. External lines (heptane, propylene, N_2/vacuum, and catalyst injection) are attached to the reactor with quick connect fittings.

Throughout the reaction, temperature, pressure, and propylene mass flow signals are processed with an Analog Devices μMAC 4000 analog-to-digital converter and stored in a PDP 11/55 computer. Propylene flow to the reactor is measured on a 10 V scale with a Teledyne-Hastings gas mass flowmeter; mass flow is proportional to voltage. Figure 3 is a plot of raw data from a typical experiment.

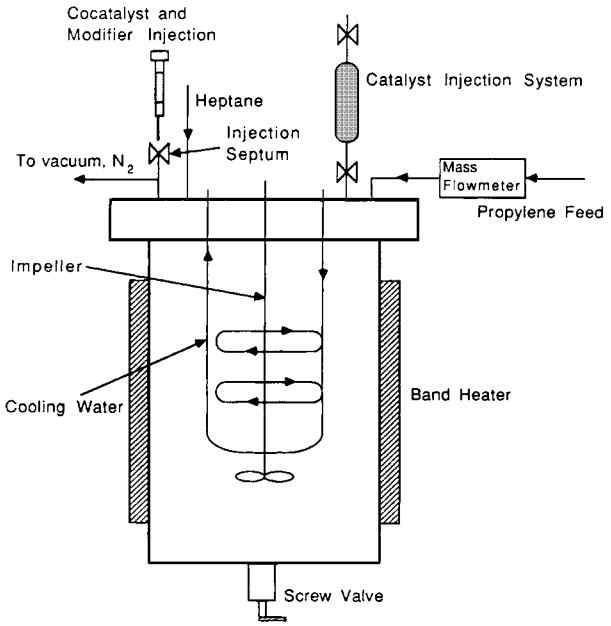

Figure 2 Schematic of reactor setup used for experimental study of propylene polymerization in heptane diluent.

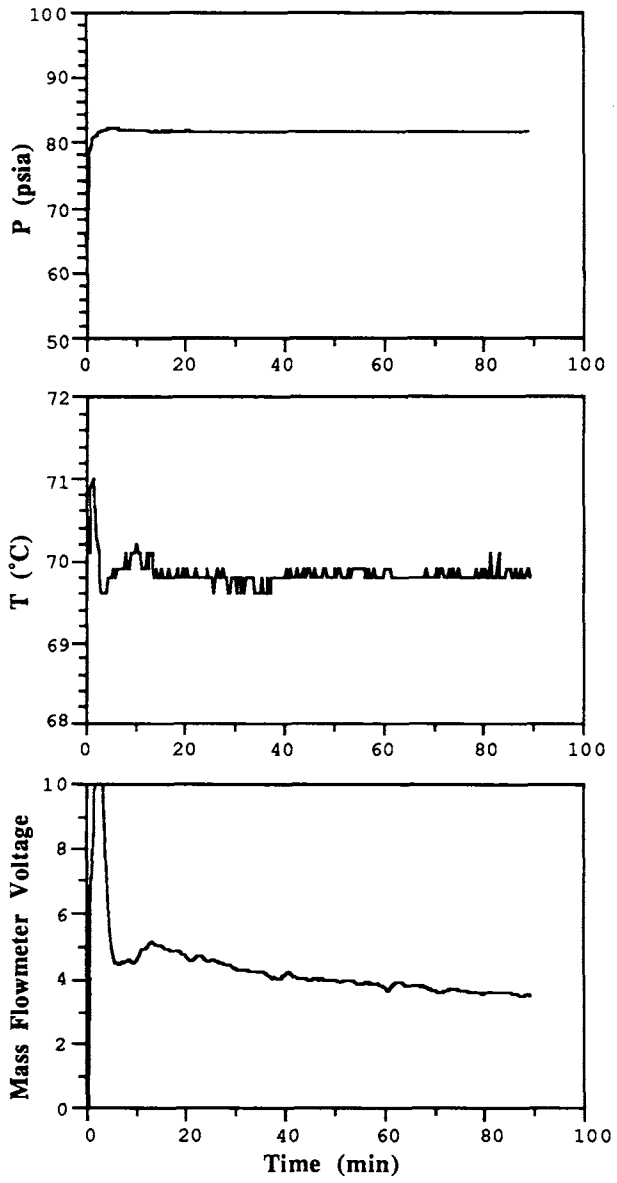

Figure 3 Typical raw data from an experimental run: Pressure, temperature and mass flowmeter voltage vs. time.

The initial spike in mass flowmeter voltage (propylene flow) is due to the final portion of reactor fillup.

Since olefin polymerization catalysts are sensitive to trace amounts of impurities, purification of reactor reagents is very important. Polygrade propylene, obtained from Phillips Petroleum, is passed through alumina and reduced copper (BASF R3-11 catalyst) to remove oxygen, water, and other oxygenated impurities. HPLC grade heptane (> 99.9% C7 alkanes, < 50 ppm water) is contacted with molecular sieves before being drained under N_2 blanket to a storage bomb in the reactor system.

The catalyst used in this study is a high activity Ti catalyst on a $MgCl_2$ support (1.84 wt % Ti). Because of its high activity, only a small amount of catalyst is needed to achieve moderate solids content in the 4-L reactor system. To accurately measure such small amounts, it is necessary to premix the catalyst in a hydrocarbon slurry. The slurries typically consist of 1 g catalyst with 100 mL liquid; for each reaction a specified amount (5–10 mL) of the slurry is transferred to the catalyst storage bomb. More consistent results are obtained when a high viscosity liquid is used to mix the slurry; an even catalyst suspension is obtained with a 80/20 volume mixture of mineral oil and heptane. The cocatalyst and modifier used in the study are triethyl aluminum (TEA) and diphenyl-dimethyoxysilane (DPMS), respectively.

The reaction procedure is as follows (see Fig. 2):

- Catalyst slurry (5–10 mL) is loaded into the catalyst bomb in an N_2 environment inside of the Vacuum Atmospheres MO40-1 glovebox (maintained at < 1 ppm of O_2 and H_2O). The amount of catalyst is measured using a syringe with a 13 gauge needle to eliminate plugging problems. The catalyst bomb is then transferred out of the glovebox and attached to the reactor system.
- The reactor is heat evacuated at 100°C for 45 min and pressure tested for leaks with N_2.
- The reactor is charged with the desired amount (1.5 L) of heptane diluent. A small amount of heptane is also fed to the line above the catalyst bomb in order to completely flush in the catalyst during injection.
- Cocatalyst (TEA) and electron modifier (DPMS) are transferred from the glovebox to the reactor in air tight syringes and injected through the injection septum. An excess amount of TEA is added to ensure that all impurities are scavenged from the reactor.
- The reactor headspace is cleared of N_2 using repeated propylene purges. The reactor is then filled with propylene to the desired startup pressure.
- The stirrer and cooling water flow is started and the reactor is allowed to reach steady state at the desired startup conditions.
- After steady state is attained, the catalyst is forced into the reactor with a pressure gradient of N_2. The presence of the heptane above the catalyst storage bomb ensures that all of the

catalyst is washed into the reactor, and prevents any entry of N_2 into the reactor headspace.

- Propylene feed to the reactor is started, with reactor pressure controlled using a precision regulator. As the propylene is consumed during reaction, the flow of replacement propylene to the reactor is measured with the Teledyne-Hastings thermal mass flowmeter.
- After shutdown, the slurry product is contacted with a small amount of methanol and cooled. The product is filtered, vacuum dried, weighed, and treated with a 0.1% antioxidant solution (butylated hydroxytoluene, or BHT).

For third generation high-activity catalyst, it is necessary to add both an aluminum alkyl and an electron donor to the reactor system. The cocatalyst activates the catalyst while the electron donor controls the stereospecificity of the active sites. TEA and DPMS are added to the reactor prior to the catalyst. It was found that as long as a minimum concentration of TEA is maintained, the level has no effect on catalyst productivity. A constant amount of 1.2 g/L heptane gives consistent results. The TEA/DPMS ratio is controlled by the amount of DPMS injected. Preliminary experimentation showed that the best combination of activity and stereospecificity is obtained at a nominal TEA/DPMS molar ratio of 25–30. At this ratio, only 1–2% of the polymer is cold heptane soluble and productivity is $\approx$ 1600 (g/g cat h) at 70°C and 7.8 atm. At higher ratios, significant amounts of atactic polymer were formed (6–12%), and at lower ratios catalyst productivity declined. Due to consumption of TEA by impurities, the actual ratio of TEA/DPMS in the reactor is less than the nominal value.

In addition to yield and instantaneous propylene consumption rates, some post-reaction polymer analysis is used to examine the effects of operating conditions on catalyst performance. Polymer melt flow is used to characterize polymer molecular weight. As specified in ASTM test D1238, the standard test for polypropylene is done with a weight of 2.16 kg at 230°C; results (in dg/min) are often referred to as melt index (MI). High load melt index (HLMI) results—melt flow at 230°C with a weight of 21.6 kg—are also reported for some samples. The melt flow ratio (MFR) is defined as the ratio of the two flows (HLMI/MI). Although melt flow is not a fundamental measure of polymer structure, it can be empirically related to the molecular weight of the polymer.[13] As molecular weight increases, the melt flow (both MI and HLMI) of the polymer decreases due to the higher melt viscosity; MFR, a measure of the relative change in viscosity with shear stress, increases.[14] Melt flow values are also affected by the MWD of the polymer. As polydispersity (M_w/M_n) increases, it is observed that melt flow at low shear (MI) decreases, whereas melt flow at higher shear (HLMI) increases.[14] Thus a broadening of MWD leads to an increase in the observed MFR.

Powder bulk density provides an indication of polymer morphology. Bulk, or apparent, density is defined in ASTM test D1895 as the weight per unit volume of a material, including voids inherent in the material as tested. For polymer powder this includes the voids within the particles as well as voids between the particles. The apparatus used in this study to measure bulk density consists of a graduated cylinder, a funnel, and a Sepor 60 Hz shaker. The powder is poured into the preweighed granulated cylinder and shaken for 1 min. After shaking, the apparent density is calculated using the observed volume and weight. Although simple, it is important that a standardized test method be used; bulk density values are sensitive to procedural variations. The bulk density values obtained in this study are typical for polymer produced with an industrial catalyst.

RESULTS

Effect of Operating Conditions

An examination of catalyst performance over a range of operating temperatures and pressures yields information about the effect of operating conditions on catalyst productivity and polymer morphology. The conditions for the experiments are as follows:

Stirring speed:	500 rpm
Amount of heptane:	1.5 L
Cocatalyst concentration:	1.2 g TEA/L heptane
TEA/DPMS molar ratio:	25
Reaction time:	90 min
Temperature (T_{rxn}):	40–80°C
Pressure (P_{rxn}):	4.4–9.2 atm
Catalyst injection conditions:	$T = T_{rxn}$, $P \approx P_{rxn}$

Results have been analyzed to determine the relationship between catalyst activity, monomer concentration, and temperature. For most catalyst systems of this nature, it is observed that the rate of

polymerization is proportional to monomer concentration and shows an exponential dependence on temperature according to

$$R_{ob} \propto [M] \exp(-E/RT) \quad (1)$$

R_{ob} is defined as the average catalyst activity (g/g cat h) based on 90-min yield. The adequacy of eq. (1) to represent the experimental data is critically examined using both the reactor monomer concentration $[M]_b$ and the estimated sorbed concentration of monomer in the polymer phase, $[M]^*$. $[M]_b$ is estimated by the Benedict–Webb–Rubin equation of state[15] assuming vapor–liquid equilibrium; $[M]^*$ is estimated using the Krigbaum–Carpenter correlation as presented in Ref. 16. Sorption thermodynamics—the solubilization of reactants in the polymer phase—control the monomer accessibility at the catalyst surface, and thus the rate of polymerization. As shown in Ref. 16, a better estimate for the intrinsic activity of the catalyst is obtained when sorbed monomer concentration is used in the analysis of data.

The relationship between observed reaction rate and monomer concentration at a constant temperature level can be represented as

$$R_{ob} = \beta_0 + \beta_1[M] \quad (2)$$

Data sets at 45, 60, and 70°C were fit to this expression. Parameter estimates are summarized in Table I; Figures 4 and 5 show the plots of R_{ob} vs. $[M]_b$ and $[M]^*$, respectively. All data fits and parameter estimates include statistically evaluated 95% confidence intervals.

An examination of the data leads to the following observations:

- The parameter β_0 is not significantly different from zero for any data set. This is as expected—with no monomer present, no polymer is produced.
- A linear relationship between R_{ob} and [M] is observed. This supports the conclusion that the reaction is first order in monomer concentration. However, any nonlinearities could be masked by the experimental scatter.
- Using sorbed monomer concentration in eq. (2) results in an increase in the β_1 (intrinsic activity) estimate by factor of 2–3. No narrowing of the confidence interval around the parameter can be observed; the data are fit equally well with $[M]_b$ and $[M]^*$.

The effect of temperature on the polymerization behavior of olefin catalysts is quite complex. In general, increasing temperature tends to increase the rate of polymerization. However, it can also affect the number of active polymerization sites and increase the rate of catalyst deactivation. Despite these complexities, many catalysts are modeled by an Arrhenius relationship. Since the rate is observed to be first order in monomer concentration, data sets run at various pressure levels (4.4, 7.8, and 9.4 atm) have been combined. The data are fit to the expression

$$\ln\left(\frac{R_{ob}}{[M]}\right) = \hat{\beta}_0 - \hat{\beta}_1\left(\frac{1000}{T} - \frac{1000}{328.15}\right) \quad (3)$$

where

$$\hat{\beta}_0 = \ln\left(\frac{R_{ob}}{[M]}\right)_{55°C}, \quad \hat{\beta}_1 = \frac{E}{R} \quad (3a)$$

Parameter estimates are summarized in Table II; the plots of $\ln(R_{ob}/[M])$ vs. inverse temperature for the data are shown in Figures 6(a) and 6(b) for $[M]_b$ and $[M]^*$, respectively.

Table I Parameter Estimates (±95% CI) for First-Order Fit of Observed Reaction Rate to Monomer Concentration

T (°C)	Number of Expts	Normalized by $[M]_b$		Normalized by $[M]^*$	
		β_0	β_1	β_0	β_1
70	13	−106 ± 233	586 ± 119 (±20%)	−205 ± 251	1784 ± 360 (±20%)
60	6	236 ± 455	379 ± 202 (±53%)	165 ± 478	1060 ± 550 (±52%)
45	5	−131 ± 255	233 ± 72 (±31%)	−198 ± 306	618 ± 214 (±35%)

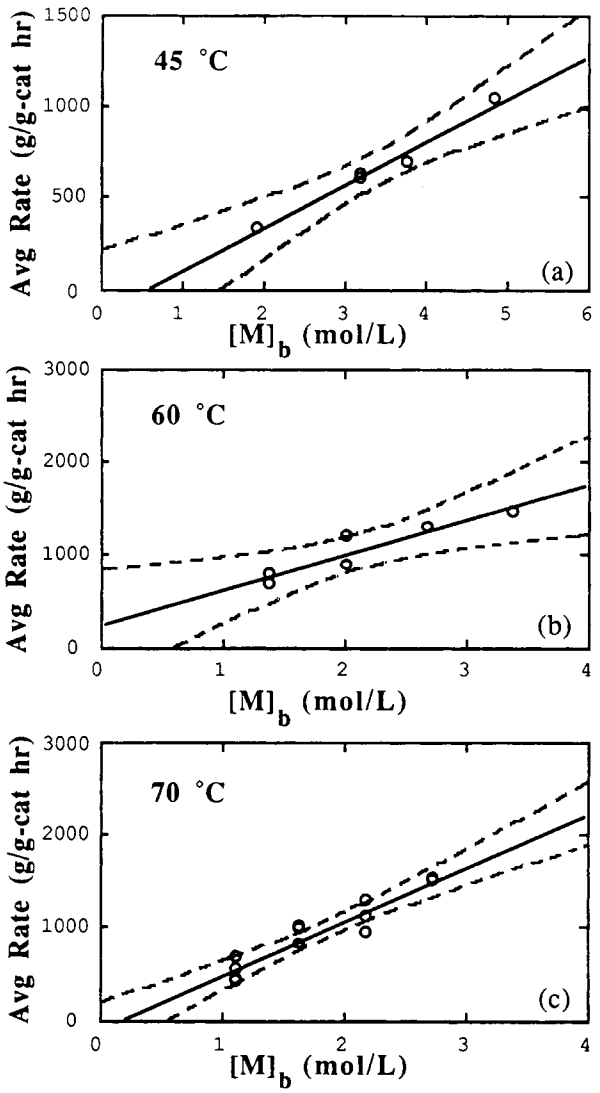

Figure 4 The relationship between reactor monomer concentration and catalyst productivity: (a) 45°C; (b) 60°C; (c) 70°C.

An examination of the data leads to the following observations:

- Normalizing the rate by [M]* results in higher estimates for both $\hat{\beta}_0$ and $\hat{\beta}_1$. The increase in $\hat{\beta}_0$ (catalytic activity) is because the ratio of [M]* to $[M]_b$ (denoted by η^*) is less than unity for polymerizations in the slurry phase. The increase in $\hat{\beta}_1$ (activation energy) is caused by the decrease in η^* with increasing temperature, as shown in Ref. 16.
- The data fit is slightly better when [M]* is used to normalize the rate. This is shown by the narrower relative confidence intervals around the parameter estimates (Table II).

All of the data points for the reactions run at 75 or 80°C fall below the predicted curves in Figure 6. This indicates a possible break in the apparent activation energy. Although the deviations are not statistically significant, other observations suggest that the experiments run at higher temperature levels need to be examined more closely. The polymer produced at 75 and 80°C has very poor morphology, with significant clumping and sticking of polymer to the reactor coils and walls observed. The sticking problems may influence the catalyst productivity and lower the observed average rate. However, the deviations may also be caused by model breakdown at this temperature level. Catalyst performance at

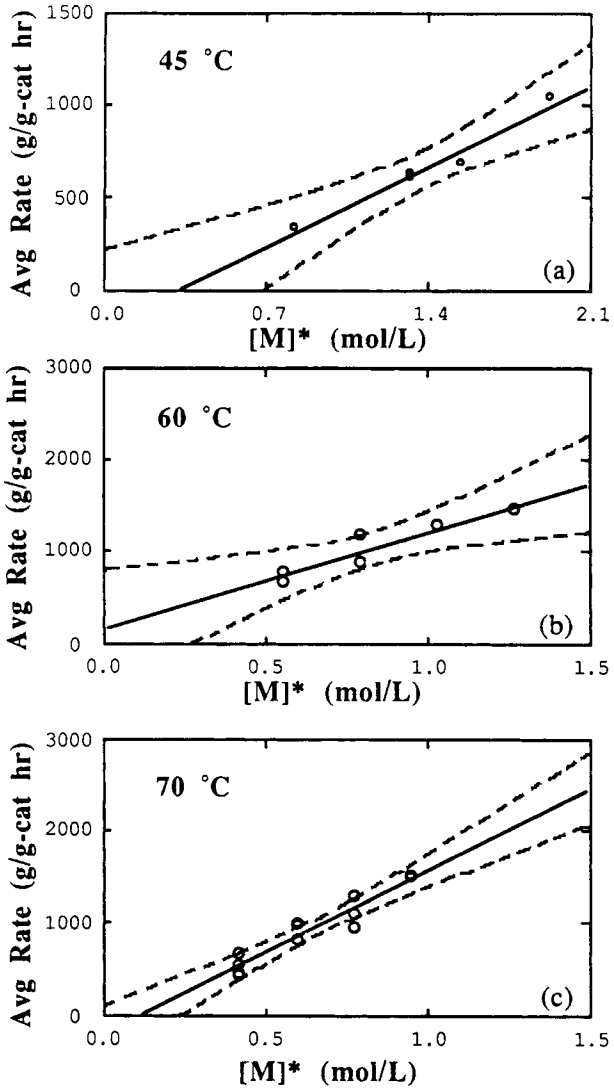

Figure 5 The relationship between sorbed monomer concentration and catalyst productivity: (a) 45°C; (b) 60°C; (c) 70°C.

Table II Parameter Estimates (±95% CI) for Fit of Data Sets to Arrhenius Temperature Relationship

		Parameters			
Analysis	Number of Expts	$\hat{\beta}_0$	$\hat{\beta}_1$	E_{act} (kcal/mol)	R_{ob} (g/g cat h), 55°C, 7.8 atm
Based on $[M]_b$: all data	27	5.852 ± 0.084 (±1.4%)	5.26 ± 0.71 (±13.3%)	10.5 ± 1.4 (±13.3%)	1040 ± 90 (±8.4%)
Based on [M]*: all data	27	6.802 ± 0.080 (±1.2%)	5.88 ± 0.66 (±11.1%)	11.7 ± 1.3 (±11.1%)	1060 ± 90 (±8.0%)
Based on $[M]_b$: rxns at $T \leq 70$°C	23	5.904 ± 0.071 (±1.2%)	6.04 ± 0.67 (±10.8%)	12.0 ± 1.3 (±10.8%)	1090 ± 80 (±7.1%)
Based on [M]*: rxns at $T \leq 70$°C	23	6.847 ± 0.069 (±1.0%)	6.55 ± 0.65 (±10.0%)	13.0 ± 1.3 (±10.0%)	1110 ± 80 (±6.9%)

the higher temperature levels is examined in more detail in the following section.

Because of the problems observed with reactions run at temperatures above 70°C, the data sets were refit to eq. (3) omitting the high temperature data points. Results are also summarized in Table II, and shown in Figure 7. Despite the loss of information caused by the deletion of the points, the uncertainty

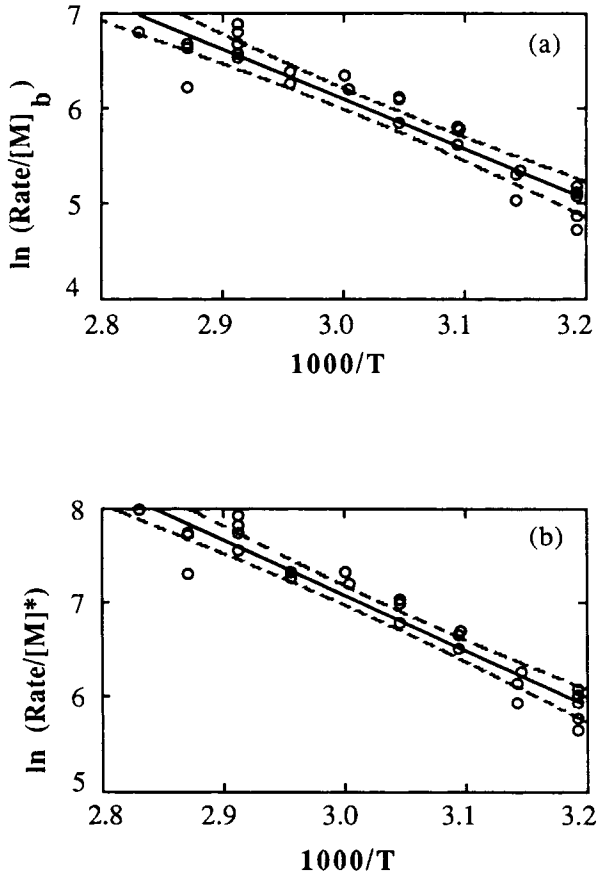

Figure 6 Arrhenius plots for complete data set: (a) rate normalized by $[M]_b$; (b) rate normalized by [M]*.

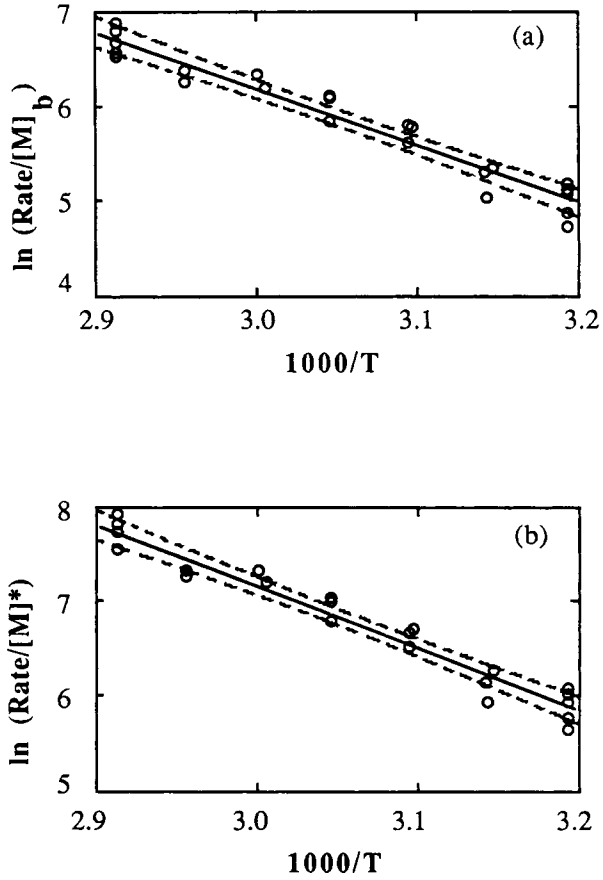

Figure 7 Arrhenius plots for reactions at $T \leq 70$°C: (a) rate normalized by $[M]_b$; (b) rate normalized by [M]*.

in the parameter estimates decreases. Although the estimates for $\hat{\beta}_0$ (activity at 55°C) do not change greatly, the $\hat{\beta}_1$ estimates (observed activation energy) increase by 10–20%. The improved data fit is also evident by an examination of residual plots for Figures 6 and 7, shown in Figure 8. When all of the data points are included, there is definite nonrandomness seen in the residuals [Fig. 8(a), (b)]. When the data points at 75 and 80°C are excluded, the residual plots show no trend with temperature [Fig. 8(c), (d)].

The material presented so far in this section has concentrated on trends observed through an examination of the average rates of polymerization calculated from the 90-min yield. By examining instantaneous rates of polymerization, it is possible to estimate the rate of catalyst deactivation. Such an estimate is semiempirical in nature, since the observed decay may be confounded by mass transfer effects.[17] Deactivation has been examined in detail by many investigators, and is usually attributed to the loss of active polymerization sites, either by poisoning or atomic restructuring of the site. Typical rate curves for reactions run under a range of conditions are shown in Figure 9. Because of the transients in propylene flow caused by slight temperature and pressure fluctuations during startup it is difficult to analyze the curves; a true measure of the instantaneous rate does not begin until about 10 min into the reaction. However, for this catalyst there is no observable effect of reaction operating conditions on the rate of decay. This is illustrated further in Figure 10, a plot of maximum against average rates of polymerization for reactions run at all temperature and pressure levels. The maximum rates are estimated by extrapolating rate curves to zero time; average rates are calculated from 90-min yield. The data are well represented by a straight line of slope 1.14.

As with free radical polymerization, polymer chain length for this system is determined by the ratio of propagation to chain termination rates.

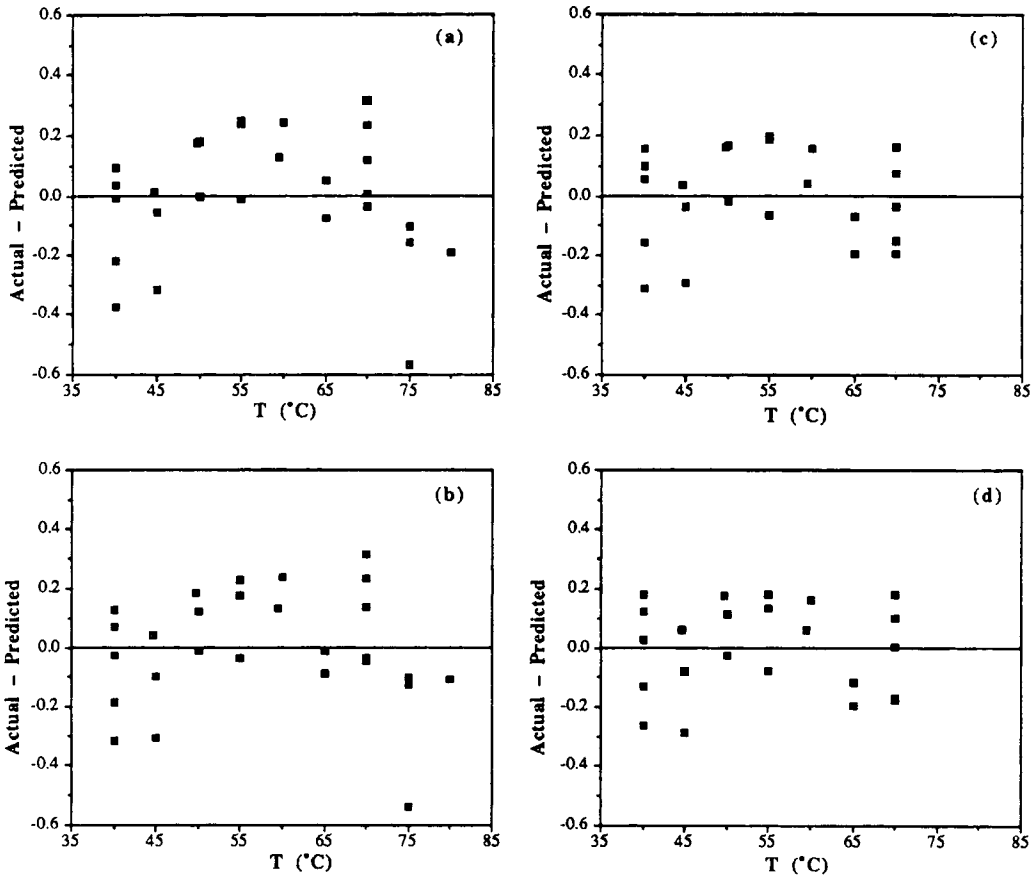

Figure 8 Residual plots (actual–predicted) for Figures 6 and 7: (a) rate normalized by $[M]_b$—complete data set; (b) rate normalized by [M]*—complete data set; (c) rate normalized by $[M]_b$—reactions at $T \leq 70$°C; (d) rate normalized by [M]*—reactions at $T \leq 70$°C.

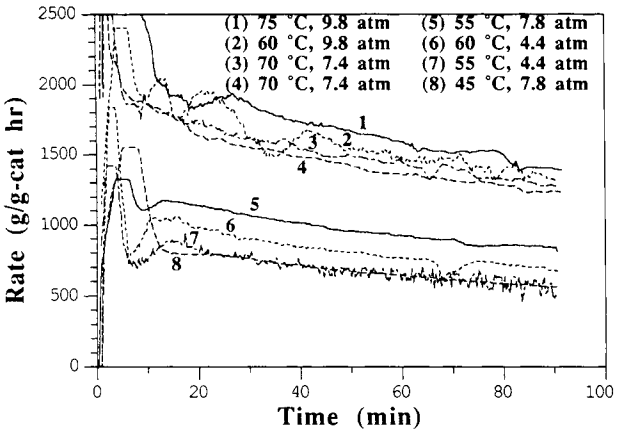

Figure 9 Catalyst production vs. time: instantaneous rate curves.

Since no chain transfer agent is used in this study, the mechanisms to consider are spontaneous termination, termination by monomer, and termination by aluminum alkyl.[18,19] Thus,

$$\frac{1}{M_n} = \frac{k_{tr}^{M}}{k_p} + \frac{1}{k_p[M]}\left(k_{tr}^{Al}[Al]^n + k_{tr}^{s}\right) \qquad (4)$$

where k_{tr}^{M} is the rate constant for transfer to monomer, k_{tr}^{Al} is the constant for transfer to TEA, and k_{tr}^{s} is the spontaneous termination constant. The exponent n is usually assumed to be 0.5. As a rule of thumb, k_{tr}^{Al} is roughly ten times greater than k_{tr}^{M}; at normal operating conditions k_{tr}^{s} is insignificant.[19] At constant temperature and alkyl concentration, eq. (4) can be written as

$$\frac{1}{M_n} = a + b\left(\frac{1}{[M]}\right) \qquad (5)$$

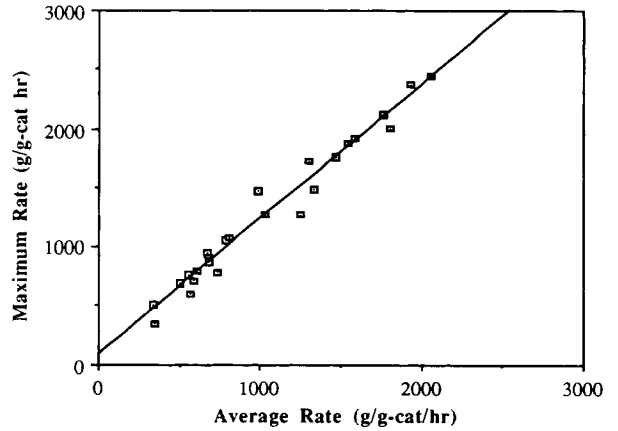

Figure 10 Catalyst maximum activity vs. 90 min average activity.

Since melt flow is inversely related to M_n, both MI and HLMI should decrease with increasing monomer concentration. This is observed experimentally, as shown in the plots of MI and HLMI vs. [M]*, Figures 11(a) and 12(a), respectively.

The effect of temperature on melt flow is shown in Figures 11(b) and 12(b) at temperature levels above 70°C ($1000/T < 2.9$), MI and HLMI values begin to increase very rapidly. Since rate constants increase exponentially with inverse temperature, this type of nonlinear response is expected. Monomer concentration decreases with increasing temperature; this also leads to higher MI at increased temperature. Melt flow values are highest for polymer formed at high temperature, low pressure operating conditions. The combined effect of all parameters on M_n depends on their relative importance according to eq. (4). The experimental results suggest that the chain transfer rate constants are more temperature dependent than the propagation rate constant. This has also been observed by others.[20,21]

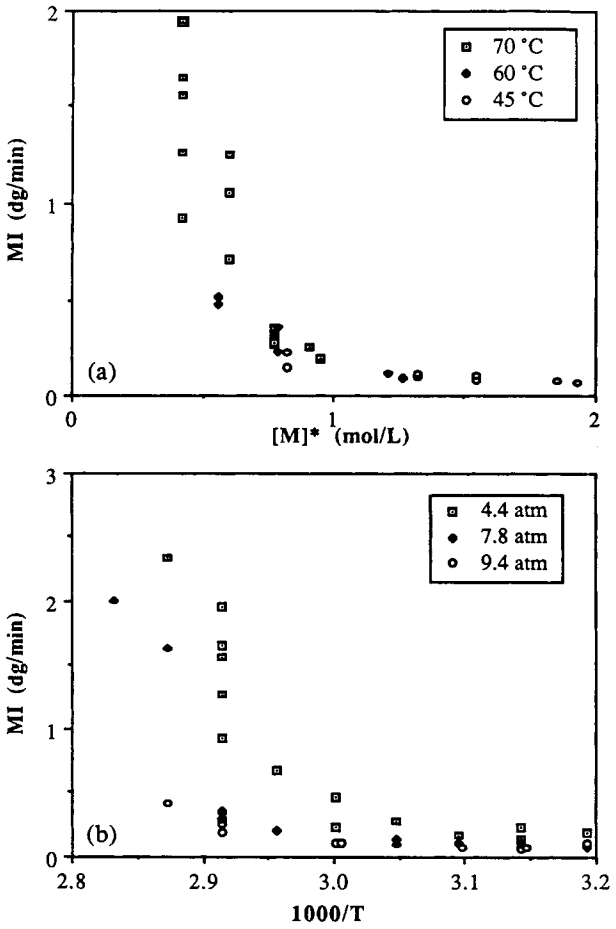

Figure 11 MI (melt index) as a function of: (a) sorbed monomer concentration; (b) inverse temperature.

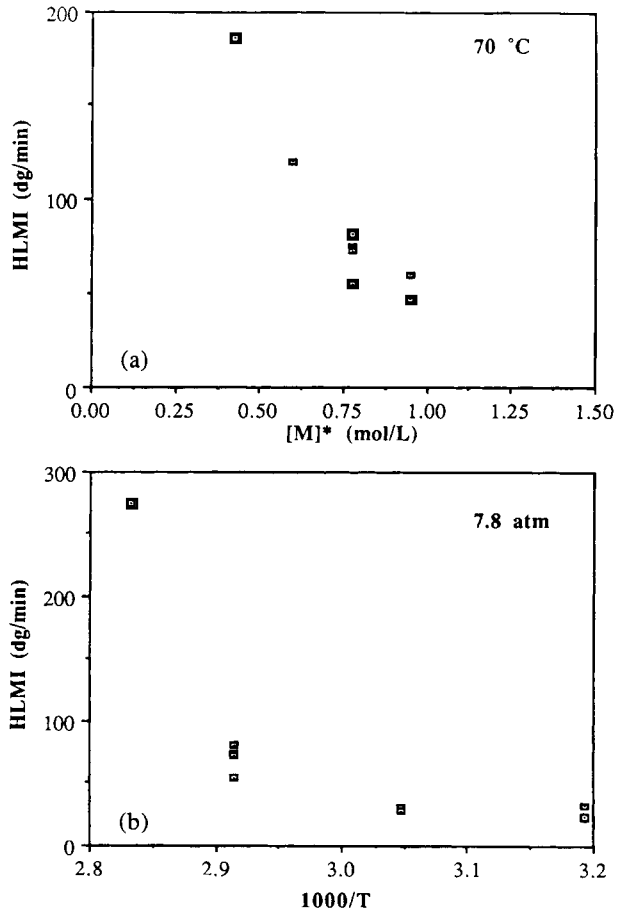

Figure 12 HLMI (high load melt index) as a function of: (a) sorbed monomer concentration; (b) inverse temperature.

In Figure 13, the effects of monomer concentration and reaction temperature on MFR are shown. At constant temperature, an increase in monomer concentration leads to an increase in MFR. As mentioned previously, this increase indicates a broadening of the MWD of the polymer. The effect of temperature on MFR is less evident—as seen in Figure 13(b) MFR decreases slightly with increasing temperature. This trend is more clearly seen with the data presented in the next section, and has also been observed with other catalytic systems.[22,23]

Figure 14 plots powder bulk density (ρ_{bulk}) as a function of monomer concentration and reaction temperature. At 45 and 60°C monomer concentration has no effect on ρ_{bulk} [Fig. 14(a)]. However, at 70°C, bulk density decreases slightly with decreasing monomer concentration. At constant pressure, Figure 14(b) shows that ρ_{bulk} is relatively constant as temperature is increased from 45 to 65°C. However, a decrease in ρ_{bulk} is seen at $T \geq 70$°C, especially at 4.4 atm. Both Figures 14(a) and 14(b) indicate that the lowest ρ_{bulk} is observed when polymer is formed at operating conditions of high temperature and low pressure. This result agrees with observations by other researchers. Tang[11] and Kim and Woo[24] observe a decrease in ρ_{bulk} as polymerization temperature increases, while Petkov and Komitov[25] show decreasing ρ_{bulk} with decreasing monomer concentration. The decrease of ρ_{bulk} at high temperatures is aggravated by the sticking problems observed in the reactor; the polymer clumps formed are fluffy and porous, and influence the bulk density of the overall sample.

Effect of Startup Conditions

The above results indicate that catalyst performance in the reactor system breaks down at temperatures above 70°C. Polymer produced at the higher temperatures is of poorer quality, as shown by a lower bulk density and by polymer caking on the coils and walls. Lower than expected reaction rates are also

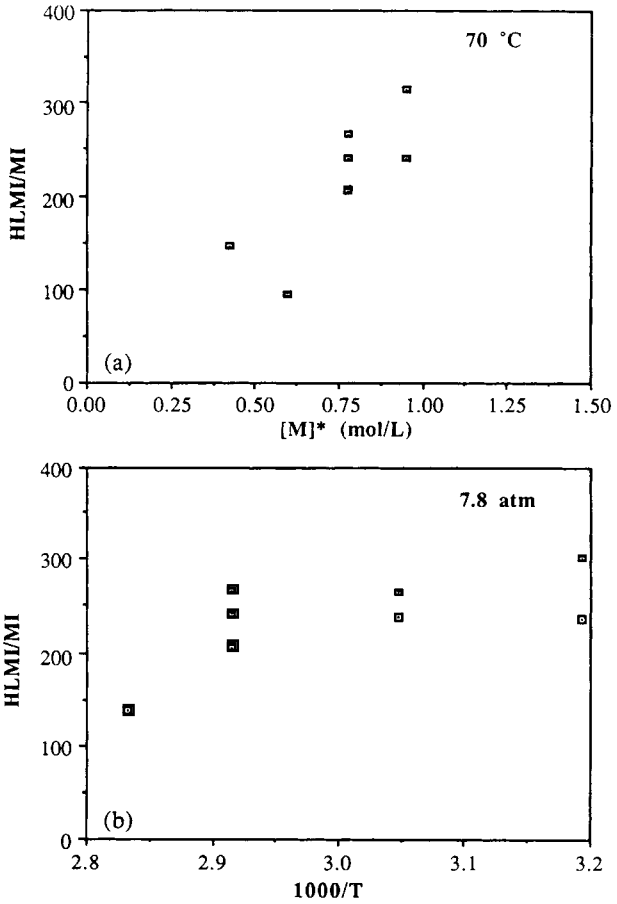

Figure 13 MFR (melt flow ratio) as a function of: (a) sorbed monomer concentration; (b) inverse temperature.

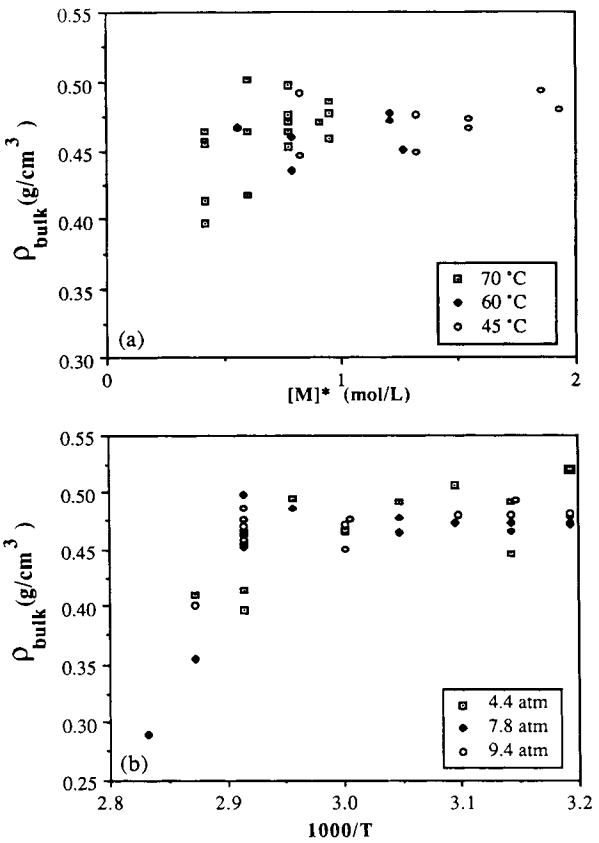

Figure 14 Bulk density as a function of: (a) sorbed monomer concentration; (b) inverse temperature.

observed; the data are better represented by the Arrhenius law when the high temperature points are excluded. Since it is desirable to produce polymer at high rates of production (i.e., at high temperatures) without losing product quality, the experimentation described in this section concentrates on this regime.

For the experiments described in the previous section, bulk density is measured on the total sample, including any polymer which may have been stuck on the reactor walls. Thus, it is not clear whether the lower values are a result of the poor product alone, or a property of the total polymer sample. The polymer analysis has been modified for the reactions described in this section; the caked polymer is removed and weighed separately from the "good" polymer slurried in the heptane phase. This allows the quantification of "poor" product (as a percentage of total yield), and makes it possible to perform analysis (bulk density, melt flow) on the "good" polymer alone.

As discussed in the introduction, a prepolymerization step at mild operating conditions (e.g., room temperature and atmospheric pressure) is necessary with some catalyst systems in order to obtain polymer particles with good morphology. In order to better understand this, the effects of startup conditions on catalyst performance are also examined in this section. The experimental conditions are as follows:

Stirring speed:	500 rpm
Amount of heptane:	1.5 L
Cocatalyst concentration:	1.2 g TEA/L heptane
TEA/DPMS molar ratio:	25
Reaction time:	90 min
Pressure (P_{rxn}):	7.8 atm
Temperature (T_{rxn}):	60–75°C
Catalyst injection conditions:	
Normal:	$T = T_{rxn}$, $P = P_{rxn}$
Prepolymerization:	T = 40°C, P = 2 atm

For the prepolymerization experiments, the catalyst was allowed to polymerize at injection conditions for 15 min before the reactor was stepped to the final operating temperature and pressure. The transition from prepolymerization conditions to operating conditions took about 25 min.

For this section of experimentation, six groups of experiments were run—prepolymerization and normal startups at temperatures of 60, 70, and 75°C. Table III reports the calculated means and standard deviations for the various temperature levels and startup procedures. To allow for direct comparison of the two startup procedures, the average reaction rates for the prepolymerization data sets have been corrected by the amount of polymer formed during the prepolymerization (15 min at 40°C and 2 atm) and transient ($\approx$ 25 min increase in temperature and pressure to T_{rxn} and P_{rxn}) stages. These yields, indicated in the table footnotes, were obtained in experiments where the reaction was terminated after the reactor had reached the final operating conditions.

The data have been analyzed to determine if there are significant differences between the groups. When calculating confidence intervals, it is assumed that the standard deviation comes from a single population. If each data group has n_i observations and a

Table III Results (± Standard Deviation) from Experimental Study of Prepolymerization on Catalyst Performance

Conditions			Results					
Temp (°C)	Startup	No. of Expts	R_{ob} (g/g cat h)	% Poor	ρ_{bulk} (g/cm^3)	MI (dg/min)	HLMI (dg/min)	MFR (HLMI/MI)
60	Normal	5	1480 ± 94	< 1	0.445 ± 0.012	0.18 ± 0.06	49.6 ± 10.3	288 ± 60
	Prepolym	5	1527 ± 136[a]	< 1	0.457 ± 0.009	0.15 ± 0.02	48.2 ± 7.7	315 ± 54
70	Normal	13	1593 ± 167	4	0.416 ± 0.025	0.37 ± 0.13	63.3 ± 9.8	186 ± 33
	Prepolym	11	1760 ± 186[b]	5	0.441 ± 0.017	0.39 ± 0.21	69.5 ± 17.8	181 ± 33
75	Normal	8	1626 ± 68	8	0.360 ± 0.023	0.89 ± 0.39	103.9 ± 13.6	118 ± 48
	Prepolym	7	1981 ± 230[c]	28	0.404 ± 0.018	0.87 ± 0.25	106.9 ± 13.9	125 ± 22

[a] After subtracting prepolymerization yield of 182 g/g cat.
[b] After subtracting prepolymerization yield of 269 g/g cat.
[c] After subtracting prepolymerization yield of 314 g/g cat.

standard deviation of s_i, an overall standard deviation for the k groups is calculated according to

$$s^2 = \frac{\sum_{i=1}^{k} [(n_i - 1)s_i^2]}{N - k}, \quad N = \sum_{i=1}^{k} n_i \qquad (6)$$

The following expression is used to determine whether the means of groups i and j are significantly different at a 95% confidence level[26]:

$$(\bar{x}_i - \bar{x}_j) \pm (t_{N-k,0.025})s\left(\frac{1}{n_i} + \frac{1}{n_j}\right)^{1/2} \qquad (7)$$

If the confidence interval encompasses zero, it can be concluded that groups i and j are from the same population; if it does not, the means are significantly different.

The results summarized in Table III provide quantitative support for the qualitative observations of the previous section—the percentage of poor product formed increases with increasing reaction temperature. However, contrary to what was expected, the prepolymerization stage also caused an increase in reactor fouling at higher temperatures. Figures 15 and 16 show the two extremes: Figure 15 is a photograph of the reactor coils after a 90-min reaction at 70°C with the normal startup procedure (2% poor product), while Figure 16 shows the coils after a reaction at 75°C with a prepolymerization startup (17% poor product).

Further examination indicated that formation of poor product actually begins during the prepolymerization stage. After a 15-min prepolymerization at 40°C and 2 atm followed by a temperature increase to 75°C, it can be seen that most of the low yield product is on the coils (Fig. 17). This observation suggests that poor polymer formation is not solely due to high reaction rates at high temperatures, but occurs at a combination of high temperature and low pressure. To test this hypothesis further, two reactions were run with catalyst injected at the operating conditions of 75°C and 3 atm. Despite the low rate of reaction (350 g/g cat h), 38% of the product was poor (Fig. 18).

During the transition from prepolymerization startup (40°C, 2 atm) to final operating conditions, the temperature is first raised to T_{rxn}, followed by an increase in pressure to 7.8 atm. This procedure minimizes the amount of polymer formed during the transition period. Two reactions were run with the transition taking place in the reverse order—the pressure was increased to 7.8 atm followed by the temperature increase to 75°C. For these two reactions, the amount of poor product was only 5%. This supports the conclusion that the poor product formation occurs at high-temperature, low-pressure operating conditions. Figure 11 indicates that the combination of high temperature and low pressure are the conditions at which polymer of the lowest molecular weight (highest melt flow) is formed. It is hypothesized that this low molecular weight product results in stickier particles which become affixed to the reactor internals.

The effects of temperature on reaction rate, bulk density and melt flow properties summarized in Table III also support the conclusions presented earlier. It can clearly be seen that ρ_{bulk} decreases with increasing temperature. Since only the density of the "good" polymer powder is measured it can be con-

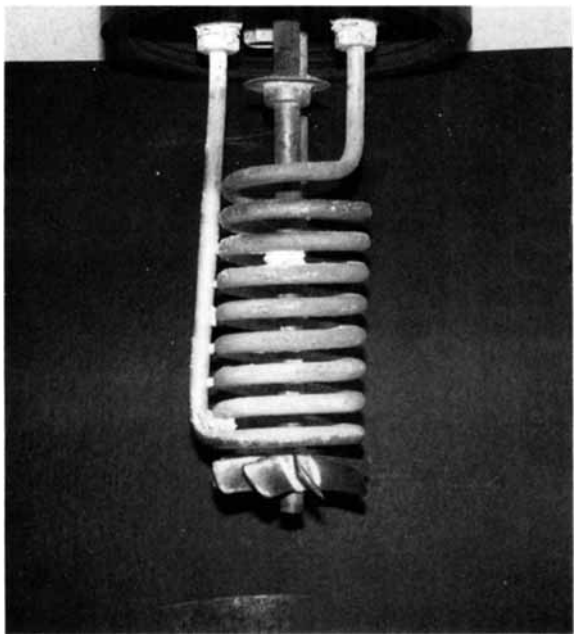

Figure 15 Photograph of reactor coils after 90 min reaction at 70°C and 7.8 atm: normal startup procedure.

cluded that this result is not an artifact caused by the formation of polymer clumps on the reactor internals. MI and HLMI increase with increasing temperature, but their ratio (MFR) decreases as temperature increases. These results also corroborate the trends discussed previously; an increase in reactor temperature causes a decrease in polymer molecular weight and a narrowing of MWD.

The average reaction rates tabulated in Table III have been used to estimate activation energies for the temperature range of 60–75°C. In this narrow range, an activation energy of 8.1 kcal/mol is estimated when [M]* is used to normalize the rate data for the reactions conducted with normal startups. For the prepolymerization reactions, the estimated value is 10.5 kcal/mol. These values are significantly lower than the estimate of 13.0 kcal/mol for the range 40–70°C (see Table II). Thus it can be concluded that eq. (3) does not adequately represent the experimental system over the complete temperature range. As discussed by Floyd et al.,[17] curvature in Arrhenius plots have been observed by numerous workers, and may be caused by activated catalyst decay or increased mass transfer resistance at the higher temperatures.

The experiments summarized in Table III show the effects of startup procedure on the polymerization process. Based on a statistical analysis, the following conclusions can be made:

- Prepolymerization has no observable effect on polymer melt flow properties. No significant difference can be seen when comparing MI, HLMI, and MFR at all temperature levels.
- At 60°C, there is no difference between the bulk density of polymer produced with a normal startup procedure compared with the prepolymerization startup. At 70 and 75°C, the bulk density of polymer produced with prepolymerization is significantly higher.
- At 70 and 75°C, prepolymerization leads to an observable increase in reaction rate. At 60°C, no significant increase in rate is observed.

These results clearly indicate that prepolymerization is an effective means of extending the operating range for polyolefin production. It is possible to increase polymer production rate through higher temperature operation while still maintaining good powder morphology.

DISCUSSION

In this paper, a complete study of the effect of operating temperature and pressure on the performance of an industrial high activity catalyst for propylene polymerization has been presented. Since the goal of this work is to better understand the influence of operating conditions on particle growth and

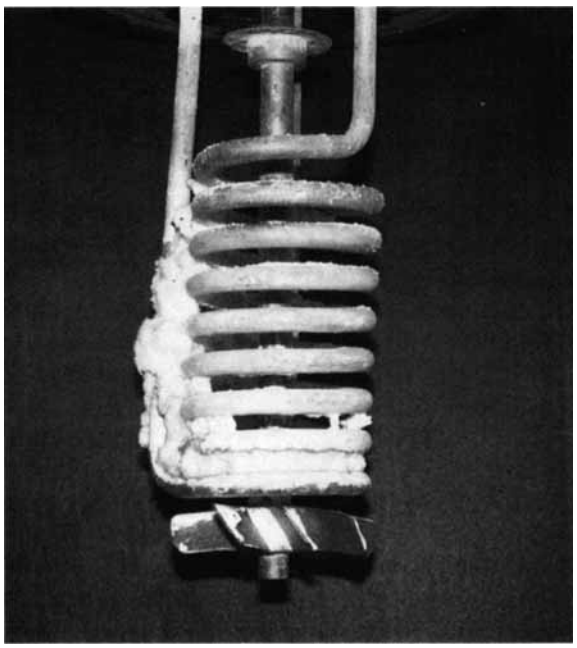

Figure 16 Photograph of reactor coils after 90 min reaction at 75°C and 7.8 atm: prepolymerization startup procedure.

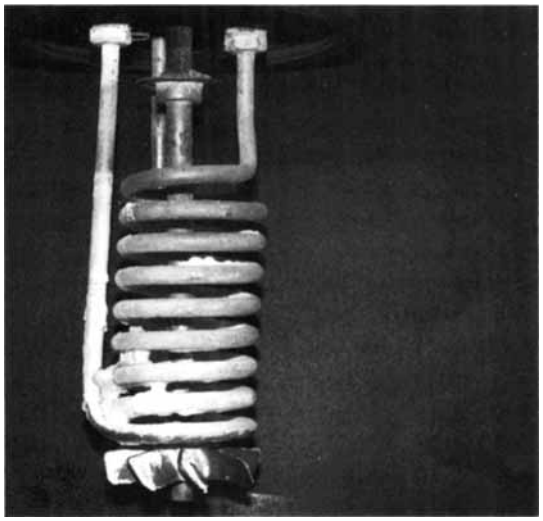

Figure 17 Photograph of reactor coils after prepolymerization startup procedure at 75°C.

morphology, this discussion will focus on this aspect of the experimental study. The following results can be summarized:

- Polymer bulk density decreases with increasing operating temperature. The combination of high temperature and low pressure results in even lower bulk density and more sticking problems in the reactor.
- Prepolymerization is an effective means of increasing product bulk density. This step allows polymerization to be performed under harsher operating conditions.

Polymer bulk density can decrease as a result of two factors—increased void fraction within the particles and increased voids between particles. The packing of particles (i.e., interparticle voids) is a function of particle shape and size distribution.[27] For a particular catalyst system, a change in interparticle void fraction during reaction implies a loss of replication. This can be caused either by the production of polymer fines through macroparticle fracture, or loss of particle shape. The formation of particle fines has been observed by Tang[11] as polymerization temperature increases, with a corresponding decrease in ρ_{bulk}. The data of Kim and Woo,[24] however, show no change in the shape of particle size distributions with temperature, even though a decrease in ρ_{bulk} with increasing temperature is observed. This indicates that the decrease in ρ_{bulk} is caused by increased voids within the particles. There was no visual evidence of loss of particle shape or production of fines for samples from this study.

An increase in intraparticle void fraction can also lead to a decrease in observed bulk density. As shown by Floyd et al.[17] mass transfer limitations within the particle are more severe as the rate of polymerization increases. For a fixed catalyst system and polymerization time, a decrease in monomer concentration at constant temperature causes intraparticle gradients to be more severe because the particle remains in the mass transfer limited regime longer. At the combination of high temperature and low pressure, mass transfer limitations within the particle are the greatest. It is precisely under the same conditions at which the lowest polymer bulk density is observed.

Tang,[11] Kim and Woo,[24] and Mkyrtchyan et al.[28] have all hypothesized that intraparticle diffusion limitations may lead to the increased formation of voids within the growing particle. A pictorial representation is shown in Figure 19, taken from Mkyrtchyan et al.[28] With no mass transfer limitations, uniform polymer growth across the radius leads to a uniformly dense polymer particle, shown schematically as Path I. Mass transfer limitations lead to nonuniform growth (Path II) within the macroparticle; the stresses of the uneven growth lead to the formation of voids within the polymer particle.

The relationship between polymer morphology and mass transfer limitations is also illustrated by examining the effects of polymerization time on particle morphology. Tang[11] shows an increase in

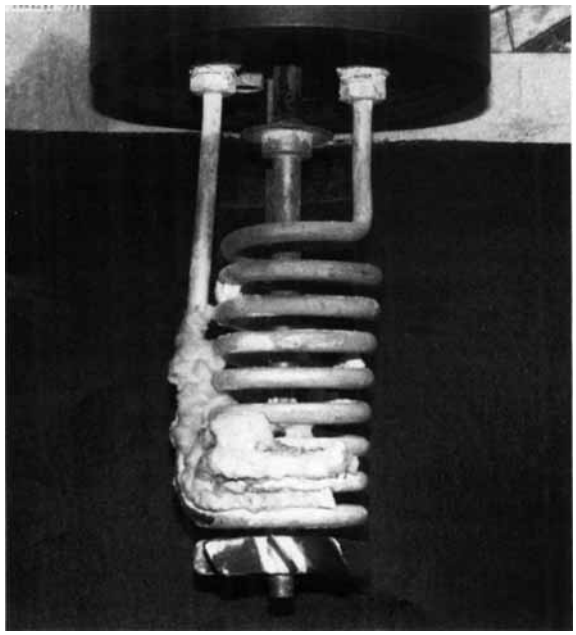

Figure 18 Photograph of reactor coils after 90 min reaction at 75°C and 3.0 atm: normal startup procedure.

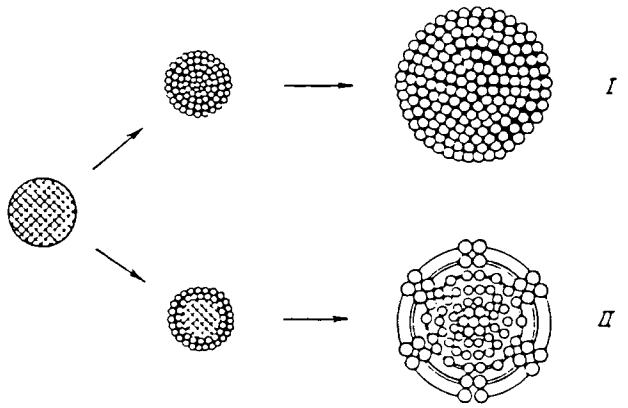

Figure 19 Particle growth mechanisms as suggested by Mkyrtchyan et al.[28]

polymer bulk density with increasing time; Bukatov et al.[7] use mercury porosimetry to measure a decrease in intraparticle void fraction with increasing time. Correspondingly, it has been shown by Floyd and co-workers[17] that mass transfer limitations are most severe during the initial stages of particle growth. This result explains the effectiveness of prepolymerization as a means of controlling particle morphology. By starting the polymerization under mild operating conditions, intraparticle mass transfer limitations are eliminated during the critical early period of polymer growth. The particle grows to a sufficient size so that mass transfer limitations are insignificant even at the harsh operating conditions encountered in the second stage of polymerization.

The experimental evidence presented in this paper supports the hypothesis that final polymer morphology is closely linked to mass transfer limitations within the growing particle. The development of a mathematical representation of this relationship and comparisons of model predictions with experimental trends will be presented in a future article.

We are grateful to the National Science Foundation and to the industrial sponsors of the University of Wisconsin Polymerization Reaction Engineering Laboratory for research support. One of the authors (R. A. H.) would also like to thank the Natural Sciences and Engineering Research Council for Canada for financial support.

REFERENCES

1. U. S. Pat. 3,530,107 (1970), to Mitsui Toatsu.
2. U. S. Pat. 4,186,107 (1980), to Hercules.
3. I. D. Burdett, paper presented at AIChE National Meeting, Washington, 1988.
4. P. Galli, paper presented at SPE RETEC Meeting, Houston, 1989.
5. C. W. Hock, *J. Polym. Sci. A-1,* **4,** 3055 (1966).
6. J. Wristers, *J. Polym. Sci. Polym. Phys. Ed.,* **11,** 1619 (1973).
7. G. D. Bukatov, V. I. Zaikovskii, V. A. Zakharov, G. N. Kryukova, V. B. Fenelonov, and R. V. Zagrafskaya, *Polym. Sci. USSR,* **24,** 599 (1982).
8. U. S. Pat. 4,210,738 (1980), to Solvay & Cie.
9. B. E. Wagner and F. J. Karol, paper presented at SPE RETEC Meeting, Houston, 1989.
10. I. G. Carson, *Angew. Makromol. Chem.,* **161,** 145 (1988).
11. S. Tang, *Catalytic Polymerization of Olefins,* T. Keii and K. Soga, Eds., Kodansha, Tokyo, 1986, p. 165.
12. U. Zucchini, G. A. Saggese, I. Cuffiani, and G. Foschini, *Transition Metal Catalyzed Polymerizations,* R. P. Quirk, Ed., Cambridge University Press, New York, 1988, p. 450.
13. J. Ross, *J. Polym. Sci. Polym. Chem. Ed.,* **22,** 2255 (1984).
14. R. L. Combs, D. F. Slonaker, and H. W. Coover, *J. Appl. Polym. Sci.,* **13,** 519 (1969).
15. R. V. Orye, *Ind. Eng. Chem. Proc. Des. Dev.,* **8,** 579 (1969).
16. R. A. Hutchinson and W. H. Ray, *J. Appl. Polym. Sci.,* **41,** 51 (1990).
17. S. Floyd, T. Heiskanen, T. W. Taylor, G. E. Mann, and W. H. Ray, *J. Appl. Polym. Sci.,* **33,** 1021 (1987).
18. G. E. Mann, M. S. thesis, University of Wisconsin-Madison, 1985.
19. V. A. Zakharov, G. D. Bukatov, and Y. I. Yermakov, *Adv. Polym. Sci.,* **51,** 61 (1983).
20. J. C. W. Chien, *J. Polym. Sci. A,* **1,** 425 (1963).
21. N. Kashiwa and J. Yoshikate, *Polym. Bull.,* **11,** 479 (1984).
22. H. G. Yuan, T. W. Taylor, K.-Y. Choi, and W. H. Ray, *J. Appl. Polym. Sci.,* **27,** 1691 (1982).
23. U. Zucchini and G. Cecchin, *Adv. Polym. Sci.,* **51,** 101 (1983).
24. I. Kim and S. I. Woo, *Polym. J.,* **21,** 697 (1989).
25. L. Petkov and P. Komitov, *Eur. Polym. J.,* **20,** 605 (1984).
26. G. E. P. Box, W. G. Hunter, and J. S. Hunter, *Statistics for Experimenters,* Wiley, New York, 1978, p. 203.
27. D. J. Cumberland and R. J. Crawford, *The Packing of Particles,* Elsevier, New York, 1987.
28. S. A. Mkyrtchyan, B. A. Uvarov, V. I. Tsvetkova, Yu. M. Tovmasyan, S. O. Chistyakov, G. F. Rachinskii, and F. S. D'yachkovskii, *Polym. Sci. USSR,* **28,** 2343 (1986).

Received October 20, 1990
Accepted January 3, 1991